Ultraviolet polarizer with Ge subwavelength grating

Yuusuke Takashima,[1,3,*] Masato tanabe,[2] masanobu haraguchi,[1] yoshiki naoi[1]

[1]Graduate School of Technology, Industrial and Social Science, Tokushima University, 2-1 Minami-josanjima, Tokushima, 770-8506, Japan
[2]Faculty of Science and Technology, Tokushima University, 2-1 Minami-josanjima, Tokushima, 770-8506, Japan
[3] Research Fellow of Japan Society for the Promotion of Science, Japan Society for the Promotion of Science, 5-3-1 Kojimachi, Chiyoda, Tokyo, 102-0083, Japan
*Corresponding author: takashima@ee.tokushima-u.ac.jp

A polarizer with high extinction (ER) ratio was developed in the ultraviolet wavelength region using a germanium subwavelength grating (Ge-SWG). By utilizing an eigenmode with the Ge-SWG, a high ER was numerically predicted to exist without requiring a high structural aspect ratio. After using lithography to fabricate the proposed Ge-SWG, an experimental high ER value of 17.4 dB was reached at a wavelength of 360 nm in the developed Ge-SWG, which had a very low structural aspect ratio of 1.67. © 2015 Optical Society of America

OCIS codes: (050.2770) Grating; (230.5440) Polarization-selective devices; (050.6624) Subwavelength structure.

1. INTRODUCTION

Linearly polarized ultraviolet (UV) light strongly interacts with many photo-reactive polymers and changes their chemical constitutions [1,2]. This photo-reactive chemical change is highly useful for various integrated applications, such as photo-alignment and molecular switching devices. The development of such devices requires a small-scale polarization control method and a high extinction ratio (ER), which is defined as the ratio of orthogonal polarization states.

A polarizing film composed of an iodine-doped polymer has been widely used to obtain polarized light from the visible (VIS) to infrared (IR) wavelength regions. At UV wavelengths, however, the ER of the polarizing film is insufficient for the above applications due to strong light absorption in the iodine polymer. On the other hand, a prism polarizer, such as the Glan–Thompson polarizer, shows extremely high ER in the broad wavelength region from UV to IR. However, the bulky size and the high cost of prism polarizers often cause difficulty in their practical use, making them unsuitable for integration in devices regardless of the high ER.

A type of subwavelength grating (SWG) polarizer, which is composed of a thin single-layer grating on a substrate, has been proposed to overcome these issues. A schematic diagram of a SWG polarizer is shown in Fig. 1. In the SWG structure, the eigenmodes are defined as solutions of Maxwell's equations in a periodic refractive index distribution. Interaction between the eigenmodes and incident light determines the electromagnetic response within the SWG. The interaction generates a different electromagnetic response for pairs of orthogonal polarization states, such as p- and s-polarization states, owing to their different boundary conditions. The direction of the electric field for s- and p-polarization is parallel and perpendicular to the grating grooves, respectively. High polarization selectivity can be obtained by utilizing the different interactions [3-10]. The grating structure, which is designed to have a much shorter period than the incident wavelength, is known as a "wire-grid polarizer" and is used to control the polarization state of light in the IR [11,12], VIS [13-16], UV, [17,18] and deep UV wavelength regions [19-22]. The wire-grid polarizer has a both high extinction ratio and compact design, so it is suitable for integrated polarization-controlling applications. However, the polarizer typically requires a structural aspect ratio, defined as the ratio of the grating height to ridge width, larger than 5 and a grating period of around 100 nm in the UV wavelength region [20,22]. Despite the progress in micro-fabrication techniques, the fabrication of SWGs with such a high aspect ratio and small period can be challenging.

The optical characteristics of SWGs have been estimated using effective-medium-theory (EMT) [23]. Using EMT, the SWG structure has been approximated to the optical anisotropic uniform layer with an effective refractive index. In other words, the eigenmode in the SWG was assumed to be a plane wave. Although this approach is a powerful and useful design method for SWGs, the approximation is only accurate when the grating period is much shorter than the incident wavelength [15, 24]. Moreover, the grating period was generally decreased as much as possible in order to obtain high ER. The resultant design requires a very small period for the SWG, which induces difficulty in the fabrication process.

Analysis of the electromagnetic response of eigenmodes due to the periodic refractive index distribution has been studied in the IR wavelength region [25]. This analysis has been employed for the dielectric SWG using only the real part of the refractive index. However, the optical characteristics of the mode in the UV wavelength region differed from those in IR wavelength region because the imaginary part of the SWG materials becomes large. We have recently shown the effects of the imaginary part of the refractive index on the SWG polarization characteristics [26].

In this study, we developed a UV polarizer utilizing the eigenmode in Ge-SWG with a very low structural aspect ratio of 1.67. We calculated the

electromagnetic field distribution in the SWG using the finite-difference time-domain (FDTD) method in order to discuss and characterize the optical properties of the eigenmode as a polarizer in UV wavelength region. The fabricated Ge-SWG with the structural aspect ratio of 1.67 experimentally demonstrated a very high extinction ratio of 17.4 dB in the UV wavelength region without a significant decreasing of the light intensity.
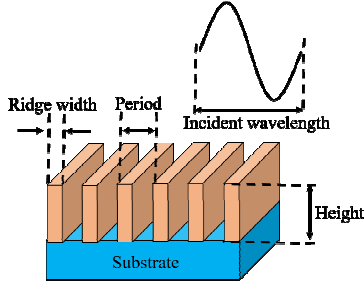

Fig. 1. Schematic diagram of a SWG polarizer

2. THEORETICAL INVESTIGATION OF THE SWG EIGENMODES

The interaction between the eigenmode and incident light determines the electromagnetic response within the SWG. The number of exited modes and their propagation constants strongly depend on both the period (Λ) and the filling factor (ff), which is defined as the ratio of the ridge width (w) to the grating period [7,25]. If the grating material has a light absorption coefficient, namely the imaginary part of the refractive index, the propagation constant of the mode is a complex number. The real and imaginary parts of the propagation constant determine the phase and decay of the mode, respectively.

In our previous report, we theoretically investigated the complex propagation constant of the eigenmode in SWGs composed of various materials with complex refractive indices [26]. Based on the results of our previous study, we chose Ge for the SWG material in the present study. The filling factor and grating height (H) were set to ff = 0.6 and H = 100 nm, respectively, to produce a SWG with high polarization selectivity in the UV wavelength region without a significant decrease in the light intensity.
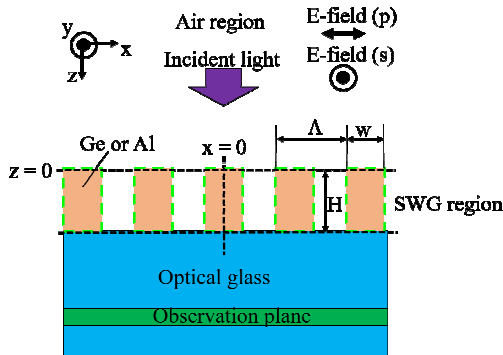

Fig. 2. Schematic model of the SWG in the FDTD calculation

We theoretically surveyed the electromagnetic distribution using the FDTD method to estimate the optical characteristics of a Ge-SWG as a UV polarizer. The optical characteristics of an Al-SWG were also estimated because Al has generally been used for wire-grid polarizers. Figure 2 shows the schematic model of SWGs used in the FDTD calculation. The green dashed squares in Fig. 2 represent the grating ridges, and the area surrounded by the dashed black lines show SWG

region. In this model, Ge and Al ridges were arranged on the optical glass with period Λ. The ridges in this model were assumed to have a rectangle shape. The complex refractive index values of Ge, Al, and optical glass were 4.0476+2.6184i, 0.38857+4.3375i, and 1.5486+0i, respectively [27,28]. The incident plane wave normally entered the SWG with a wavelength of 360 nm, and the light propagated in the +z direction in the air to glass region. The transmitted light intensity for the p- and s-polarizations was evaluated using the Poynting vector at the observation plane in Fig. 2. Other calculation conditions can be obtained from our previous report [26].

Figure 3 (a), (b), and (c) show the calculated transmission for p-polarization, the calculated transmission for s-polarization, and the ER as a function of the ratio of incident wavelength to the grating period (λ/Λ), respectively. The period Λ of the grating was changed with a constant incident wavelength of 360 nm. The ER is defined by

$$ER = 10 \log_{10} \frac{T_p}{T_s} \qquad \textbf{(1)}$$

where T_p and T_s are the transmissions for the p- and s-polarizations, respectively. The inset in Fig. 3(b) shows the s-polarized light transmission in the region from λ/Λ = 2 to 4. These figures show that the transmission dependence on λ/Λ considerably differs between the p- and s-polarizations in both SWG cases. With increasing λ/Λ, the transmission for p-polarized incident light became much larger than that for s-polarization. In both Ge- and Al-SWG cases, the transmission for p-polarized light largely oscillated with increasing λ/Λ, as shown in Fig. 3(a). For s-polarization, transmission through the Al-SWG monotonically decreased with increasing λ/Λ. The tendencies have been reported in many previous reports [13,19].

In contrast, the local minimum value of s-polarized light transmission through the Ge-SWG was obtained at λ/Λ = 3.6, and the transmission increased in the region from λ/Λ = 3.6 to 4. As a result, the Ge-SWG exhibited a peak ER at λ/Λ = 3.6, where the grating period corresponds to 100 nm. The peak ER value reached almost 40 dB when 20% of the p-polarized light transmission was maintained. These values were much higher than those of the Al-SWG with the same parameters. In addition, a very low aspect ratio of 1.67 was required to obtain such a high ER.
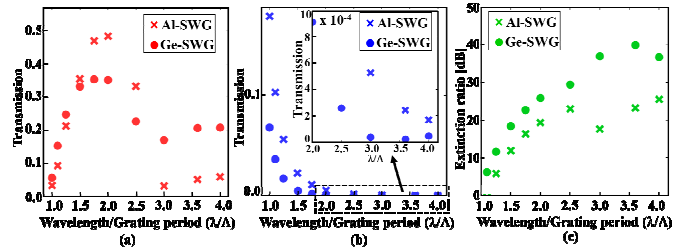

Fig. 3. Calculated transmission for (a) p-polarization (b) s-polarization and (c) the ER as a function of λ/Λ. The crosses and filled circles indicate the results for Al-SWG and Ge-SWG, respectively.

The high ER was mainly caused by the highly suppressed transmission for s-polarized light. To reveal the origin of the suppressed transmission for s-polarization, a counter map of the magnitude for the Poynting vector of the eigenmode inside the SWGs was developed with the parameter of λ/Λ = 3.6, as shown in Fig. 4. Figure 4(a) and (b) show the counter map for s-polarization inside Al-SWG, and the counter map inside Ge-SWG, respectively. Regions A and B in Fig. 4 (a) and (b) represent the grating ridge material (Al, Ge) and the air-gap in the SWG, respectively. The positive and negative values of the Poynting vector correspond to the +z and –z propagation directions, respectively. The magnitude of the Poynting vector was normalized by the magnitude of

incident light.

The counter maps of the Poynting vector in the Al- and Ge-SWGs were significantly different. In the Al-SWG, the energy of the eigenmode was evenly distributed in the ridges region (region A) and the air-gap region (region B). The counter map in Al-SWG was slightly distorted at the top side of the grating, and the optical behavior of the eigenmode can be approximated to that in homogeneous layer with an effective refractive index [22]. On the other hand, the distribution in Ge-SWG significantly differed from that in Al-SWG, and most of the mode energy was concentrated in the Ge ridges region in which light absorption existed. Thus, the energy rapidly decayed with the propagation of light, and the transmission of s-polarization in the Ge-SWG was highly suppressed.
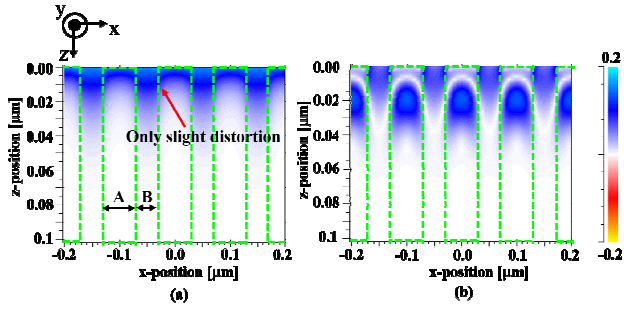

Fig. 4. Counter maps of the magnitude for the Poynting vector of the eigenmode in the (a) Al-SWG and (b) Ge-SWG for s-polarization. The Poynting vector was normalized by the magnitude of incident light. Green squares indicate the grating ridges.

For p-polarization, the transmission through the Al-SWG was higher than that through the Ge-SWG in the region from λ/Λ = 1.5 to 2.5, as shown in Fig. 3(a), regardless of the larger imaginary part of refractive index in Al than that in Ge. This indicates the absorption coefficient of the SWG ridge material is not dominant factor for the p-polarization transmission through the SWG. To investigate the transmission mechanism for p-polarization, we also calculated the counter maps of the magnitude for the Poynting vector of the p-polarized eigenmode in the Al- and Ge-SWGs with λ/Λ = 2. Figure 5(a) and (b) show the counter maps for p-polarization inside Al-SWG and Ge-SWG, respectively. Since the Poynting vector indicates the density of energy per unit area, the total energy does not exceed the incident energy despite of the Poynting vector value higher than 1. The eigenmode energy highly concentrates into the air-gaps for both Al- and Ge-SWG, compared with that for s-polarization. In Al-SWG case, about 1.3 times greater energy than that of Ge-SWG was concentrated into the air-gap. As a result, the transmittance through the Al-SWG became higher than that through the Ge-SWG, regardless of the larger refractive index imaginary part of Al than that of Ge.

These transmission mechanisms for s- and p-polarization can be understood as follows. The eigenmode states and the energy distribution within the SWG strongly reflected the special periodic distribution of the refractive index and the boundary conditions of the electromagnetic field. The boundary condition of electric field defined the transmission mechanism of the SWG, because the boundary condition of magnetic field was always satisfied at optical wavelength region (Relative permeability is nearly 1). If the real part of refractive index of the grating ridge was low (similar to that of Al-SWG), the optical behavior of the s-polarized mode approximately resembled a plane wave in a homogeneous layer with an effective index value because the mode energy evenly distributed in the SWG due to continuous of electric field at the interface between the grating ridges and air-gaps. In contrast, high refractive index modulation (similar to that of Ge-SWG) induced a

large distortion of the energy distribution in the SWG because of the difference of mode propagation velocity between grating ridge and air-gap. The optical behavior of the mode in this case was significantly different from that in the homogeneous layer, and the energy distribution strongly depended on the grating geometry. Thus, the local minimum transmission for s-polarization could only be obtained at a certain grating parameters.

The eigenmode energy for p-polarization could highly concentrate into the air-gaps because the electric field was discontinuous at the interface between the grating ridges and air-gaps. As a result, the transmission for p-polarization could be higher than that for s-polarization, and the propagation loss of the eigenmode was determined not only by absorption coefficient of the material but also by grating geometry.
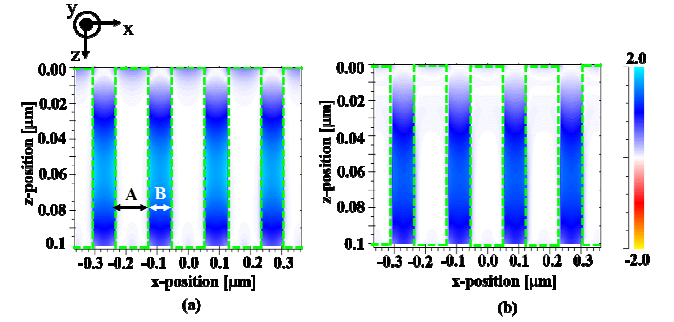

Fig. 5. Counter maps of the magnitude for the Poynting vector of the eigenmode in the (a) Al-SWG and (b) Ge-SWG for p-polarization.

These results indicated that monotonically decreasing the period was not an optimal design method for identifying high ER and high transmission, and even low aspect ratio structures could be used to realize high-performance polarizers. This insight of our design technique could be used to overcome difficulties in the fabrication process for high ER and high transmission devices, especially for polarizers in shorter wavelength regions such as the UV wavelength region.

3. EXPERIMENTAL RESULTS AND DISCUSSIONS

Based on our theoretical considerations, we fabricated a polarizer with a Ge-SWG that had a period of 100 nm, grating height of 100 nm, and ridge width of 60 nm on an optical glass substrate in order to demonstrate high ER at UV wavelengths. Then, a 120-nm-thick film of positive electron beam resist (ZEP 520A: Zeon) was spin-coated on the substrate. The area of the grating pattern was 1.2 x 1 mm². The grating pattern was drawn using electron beam lithography, and the patterned resist was developed. Then, a 100-nm-thick Ge film was thermally evaporated on the patterned resist, and the resist was removed. A scanning electron microscope (SEM) image of the fabricated Ge-SWG is provided in Fig. 6. The fabricated grating period and Ge ridge width were 100 nm and 60 nm, respectively.
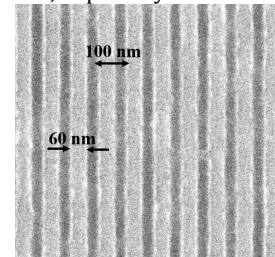

Fig. 6. SEM image of the fabricated Ge-SWG.

We measured the transmission of s- and p-polarized light thorough the fabricated Ge-SWG to evaluate the performance of the SWG as a UV polarizer. Figure 7 shows the schematic experimental set up for the evaluation. The light source was a UV light-emitting diode (UV-LED) with a peak wavelength of 360 nm, and a collimation lens was placed in the front the LED. The beam diameter was about 0.8 mm using the iris diaphragm. The polarization of the collimated light was controlled by rotating the polarizer. Incident light normally entered the Ge-SWG.
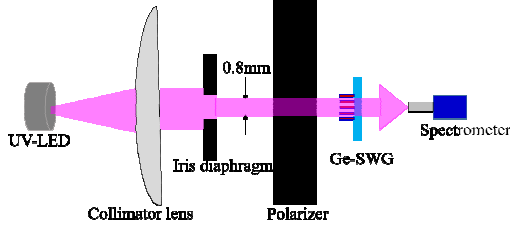

Fig. 7. Schematic of the experimental set up.

The transmitted light intensity through the fabricated Ge-SWG was measured using a spectrometer. Figure 8 shows the transmittance for p- and s-polarized incident light and ER as a function of the incident wavelength. We also showed error bars at three typical wavelengths in Fig. 8. The error bars were standard deviation over three measurements. The maximum magnitude of error bars were lower than 1 dB in the wavelength region from 340 nm to 380 nm and show that the noise level of our measurement was low enough to evaluate ER. The transmittance for p-polarized light was much higher than that for s-polarized light. The tendency of the optical characteristics of the fabricated SWG showed good agreement with that in FDTD calculation. The measured ER value reached about 17.4 dB in the 360 nm wavelength region when the p-polarization transmittance was maintained at almost 12%. However, the measured ER value was lower than the calculated value. This deviation was mainly caused by leaking s-polarized light from an imperfect region of the SWG with the fabrication error. The ER dramatically varied with a minute change in the s-polarized light. However, the measured ER value will still be acceptable for polarization control applications in the UV wavelength region, such as photo-alignment devices [1,2].
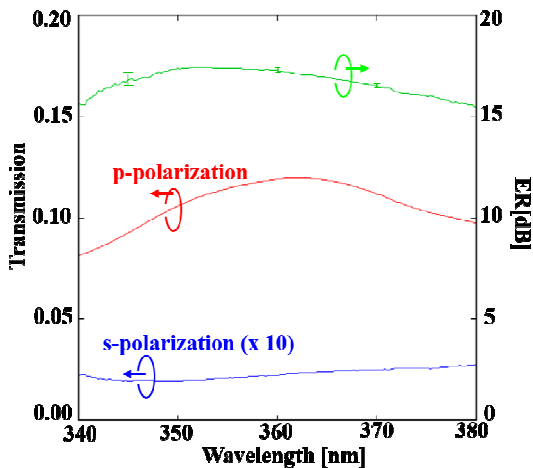

Fig. 8. Measured transmission and ER in the fabricated Ge-SWG.

We compared the optical characteristics of the fabricated Ge-SWG to those of other UV polarizers to evaluate the performance of the Ge-SWG. In particular, the ER value was compared, as this value is important for the development of UV polarization control applications. Only Al-, Ir-,

and Si-based wire-grid polarizers have been reported for the 360 nm wavelength [17,18]. An Al-based wire-grid polarizer with an aspect ratio of about 4.4 showed an ER value of about 16 dB around the wavelength of 360 nm; this ER value was lower than that in the fabricated Ge-SWG polarizer despite of the very high aspect ratio in the Al-based polarizer. Although Ir-based polarizers showed high ER values in the UV wavelength region, structural aspect ratios of almost 4 and periods on the order of 100 nm were required. Achieving both a high aspect ratio and small period is extremely challenging to fabricate. On the other hand, the Si-based wire-grid polarizer with a structural aspect ratio of about 1.9 showed an ER value of 19.5 dB at the wavelength of 365 nm. Compared with these polarizers, an ER value of 17.4 dB was successfully demonstrated using the Ge-SWG with a much lower aspect ratio of 1.67. This aspect ratio was less than half that in the Al- and Ir-based wire-grid polarizers. To best of our knowledge, the aspect ratio of 1.67 was lowest value in wire-grid polarizers that could simultaneously maintain a high ER value (> 17 dB) in the UV wavelength region. These results suggested that an ER value on the order of that obtained in Si-based wire-grid polarizers could be successfully realized regardless of the very low structural aspect ratio of 1.67 [18]. Moreover, Ge-SWG can be fabricated by very low temperature process as compared with Si-SWG. Thus, the Ge-SWG demonstrated in this work could be significant for overcoming difficulties in the fabrication process, and the Ge-SWG would be suitable for practical applications of UV polarizers due to its high ER value.
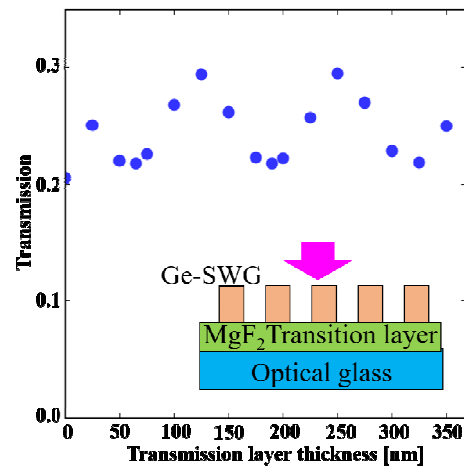

Fig. 9. Dependence of the transmission on the transition layer thickness. The insert is the SWG model in the calculation.

We theoretically discuss the improvement of the transmission for p-polarization through the Ge-SWG by Fabry-Perot interference effect due to inserting a low refractive index transition layer between the SWG and substrate [29]. In this calculation, a MaF$_2$ was employed as the transition layer owing to its low refractive index value and low light absorption in UV wavelength region. The refractive index value of MgF$_2$ was 1.3866+0i at the wavelength of 360 nm [30]. Influence of the transition layer on the transmission for p-polarization was evaluated by FDTD calculation. The period, filling factor, and height of SWG model were set to Λ = 100 nm, ff = 0.6, and H = 100 nm, respectively. The normal transmission for p-polarization is shown in Fig. 9 as a function of the transition layer thickness. In Fig. 9, the transmittance oscillated for the increasing of transition layer thickness owing to Fabry-Perot interference effect, and the maximum transmission reached to about 30 % at the wavelength of 360 nm. The transmittance value was comparable with that of conventional UV polarizing plate. This calculation result indicates that the transition layer improves the

transmission and is of great use for UV polarizer.

4. CONCLUSION

In conclusion, we experimentally demonstrate a UV polarizer by utilizing the eigenmode due to the periodic refractive index distribution of a Ge-SWG. We calculated the counter map of the magnitude for Poynting vector of the eigenmode using the FDTD method in order to estimate the performance of Ge-SWG as a UV polarizer. The calculated results indicated that Ge-SWG could be used to achieve a high ER value without significantly decreasing the UV light intensity despite its very low structural aspect ratio. The designed polarizer was fabricated using electron beam lithography, and a high ER was experimentally demonstrated with 1.67 structural aspect ratio of the SWG. The measured ER reached about 17.4 dB around a wavelength of 360 nm when about 12% of the p-polarized transmittance was maintained. Moreover, the results of FDTD calculation showed that the low refractive index transition layer between the SWG and substrate significantly could improve the transmission for p-polarization. These results provided new insight into the design of SWGs for UV polarizers and could promote the development of integrated polarization control applications in the UV wavelength region.

References

1. H. Watanabe, N. Miyagawa, S. Takahara, and T. Yamaoka, "Photo-alignment material with azobenzene-functionalized polymer linked in film," Polym. Adv. Technol. **13**, 558-565 (2002).
2. D. H. Choi and Y. K. Cha, "Photo-alignment of low-molecular mass nematic liquid crystals on photoreactive polyimide and polymethacrylate film by irradiation of a linearly polarized UV light,"Polym. Bull. **48**, 373-380 (2002).
3. S. Y. Chou and W. Deng, "Subwavelength amorphous silicon transmission grating and applications in polarizers and waveplates," Appl. Phys. Lett. **67**, 742-744 (1995).
4. L. Zhuang, S. Schablitsky, R. C. Shi, and S. Y. Chou, "Fabrication and performance of thin amorphous Si subwavelength transmission grating for controlling vertical cavity surface emitting laser polarization," J. Vac. Sci. Technol. B **14**, 4055-4057 (1996).
5. T. T. Wu, S. H. Wu, T. C. Lu, and S. C. Wang, "GaN-based high contrast grating surface-emitting lasers," Appl. Phys. Lett. **102**, 081111 (2013).
6. C. Chase, Y. Rao, W. Hofmann, and C. J. Chang-Hasnain, "1550 nm high contrast grating VCSEL," Opt. Express **18**, 15461-15466 (2010).
7. C. J. Chang-Hasanain and W. Yang, "High-contrast grating for integrated optoelectronics," Adv. Opt. Photonics **4**, 379-440 (2012).
8. Y. Takashima, R. Shimizu, M. Haraguchi, and Y. Naoi, "Polarized emission characteristics of UV-LED with subwavelength grating," Jpn. J. Appl. Phys. **53**, 072101 (2014).
9. Y. Takashima, R. Shimizu, M. Haraguchi, and Y. Naoi, "Influence of low-contrast subwavelength grating shape on polarization characteristics of GaN-based light-emitting diode emissions," Opt. Eng. **54**, 067112 (2015).
10. Y. Takashima, M. Tanabe, M. Haraguchi, and Y. Naoi, "Highly polarized emission from a GaN-based ultraviolet light-emitting diode using Si-subwavelength grating on a SiO$_2$ underlayer," Opt. Commun. **369**, 38-43 (2016).
11. J. B. Young, H. A. Graham, and E. W. Peterson, "Wire grid infrared polarizer," Appl. Opt. **4**, 1023-1026 (1965).
12. Y. Lin, J. Hu, B. Cao, M. Wang, and C. Wang, "Design and fabrication of Silicon-based linear polarizer with multilayer nanogratings operating in infrared region," Opt. Eng. **56**, 017111 (2017).
13. M. Xu, H. P. Urbach, D. K. G. de Boer, and H. J. Cornelissen, "Wire-grid diffraction grating used as polarizing beam splitter for visible light and applied in liquid crystal on silicon," Opt. Express **13**, 2303-2320 (2005).
14. J. H. Lee, Y. W. Song, J. G. Lee, J. Ha, K. H. Hwang, and D. S. Zang, "Optically bifacial thin-film wire-grid polarizers with nano-patterns of a graded metal-dielectric composite layer," Opt. Express **16**, 16867-16876 (2008).
15. X. J. Yu and H. S. Kwok, "Optical wire-grid polarizers at oblique angles of incidence," J. Appl. Phys. **93**, 4407-4412 (2003).
16. F. Schlachter, J. Barnett, U. Plachetka, C. Nowak, M. Messerschmidt, M. Thesen, and H. Kurz, "UV-NIL based nanostructuring of aluminum using a novel organic imprint resist demonstrated for 100 nm half-pitch wire grid polarizer," Microelectron. Eng. **155**, 118-121 (2016).
17. T. Weber, T. Kasebier, A. Szeghalmi, M. Knez, E. B. Kley, and A. Tunnermann, "Iridium wire grid polarizer fabricated using atomic layer deposition," Nanoscale Res. Lett. **6**, 558 (2011).
18. T. Weber. S. Kroker, T. Kasebier, E. B. Kley, and A. Tunnermann, "Silicon wire grid polarizer for ultraviolet applications," Appl. Opt. **53**, 8140-8144 (2014).
19. T. Weber, T. Kasebier, M. Helgert, E. B. Kley, and A. Tunnermann, "Tungsten wire grid polarizer for applications in the DUV spectral range" Appl. Opt. **51**, 3224-3227 (2012).
20. T. Weber, T. Kasebier, A. Szeghalmi, M. Knez, E. B. Kley, and A. Tunnermann, "High aspect ratio deep UV wire grid polarizer fabricated by double patterning," Microelectron. Eng. **98**, 433-435 (2012).
21. K. Asano, S. Yokoyama, A. Kemmochi, and T. Yatagai, "Fabrication and characterization of a deep ultraviolet wire grid polarizer with a chromium-oxide subwavelength grating," Appl. Opt. **53**, 2942-2948 (2014).
22. T. Siefke, S. Kroker, K. Pfeiffer, O. Puffky, K. Dietrich, D. Franta, I. Ohlidal, A. Szeghalmi, E. B. Kley, and A. Tunnermann, "Material pushing the application limits of wire grid polarizers further into the deep ultraviolet spectral range," Adv. Optical Mater. **4**, 1780-1786 (2016).
23. H. Kikuta, H. Toyota, and W. Yu, "Optical Elements with subwavelength structured surface," Opt. Rev. **10**, 63-73 (2003).
24. P. Lalanne, J. P. Hugonin, and P. Chavel, "Optical properties of deep lamellar gratings: A coupled Bloch-mode insight," J. Lightwave Technol. **24**, 2442-2449 (2006).
25. V. Karagodsky, F. G. Sedgwick, and C. J. Chang-Hasnain, "Theoretical analysis of subwavelength high contrast grating reflectors," Opt. Express **18**, 16973-16988 (2010).
26. Y. Takashima, M. Tanabe, M. Haraguchi, and Y. Naoi, "Theoretical investigation of polarization control in ultraviolet wavelength region using eigenmode within subwavelength grating," Opt. Rev. **24**, 80-86 (2017).
27. D. E. Aspnes and A. A. Studna, "Dielectric functions and optical parameters Si, Ge, GaP, GaAs, GaSb, InP, InAs, and InSb from 1.5 to 6.0 eV," Phys. Rev. B **27**, 985-1009 (1983).
28. A. D. Rakic, "Algorithm for the determination of intrinsic optical constants of metal films: application to aluminum," Appl. Opt. **34**, 4755-4767 (1995).
29. M. Wang, B. Cao, C. Wang, F. Xu, Y. Lou, J. Wang, and K. Xu, "High linearly polarized light emission from InGaN light-emitting diode with multilayer dielectric/metal wire-grid structure," Appl. Phys. Lett. **105**, 151113 (2014).
30. M. J. Dodge, "Refractive properties of magnesium fluoride," Appl. Opt. **23**, 1980-1985 (1984).